JACS
JOURNAL OF THE AMERICAN CHEMICAL SOCIETY
Article
pubs.acs.org/JACS

Constructing a Macromolecular $K_{3,3}$ Graph through Electrostatic Self-Assembly and Covalent Fixation with a Dendritic Polymer Precursor

Takuya Suzuki, Takuya Yamamoto, and Yasuyuki Tezuka*

Department of Organic and Polymeric Materials, Tokyo Institute of Technology, O-okayama, Meguro-ku, Tokyo 152-8552, Japan

Supporting Information

ABSTRACT: A triply *fused* tetracyclic macromolecular $K_{3,3}$ graph has been constructed through electrostatic self-assembly of a uniformly sized dendritic polymer precursor having six cyclic ammonium salt end groups carrying two units of a trifunctional carboxylate counteranions, and subsequent covalent conversion by the ring-opening reaction of cyclic ammonium salt groups at an elevated temperature under dilution. The $K_{3,3}$ graph product was isolated from the two constitutional isomers by means of a recycling SEC technique, as the hydrodynamic volume of the triply *fused* tetracyclic $K_{3,3}$ product is remarkably contracted in comparison with another isomer having a ladder form in solution.

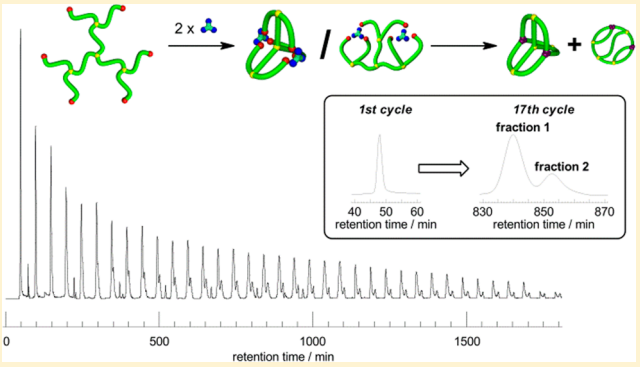

INTRODUCTION

Topologically intriguing molecular skeletons or polymer chain architectures have continuously been an attractive research subject.[1−4] Cyclic and multicyclic polymers are particularly unique from the topological viewpoint because of their elimination of chain termini in contrast to linear and branched counterparts,[4−6] and the flexible conformational motion of skeletal polymer segments between junctions and between junction−terminus coincides with a characteristic feature of the topological geometry.[4,7,8]

For the synthesis of *single* cyclic polymers, a number of effective means have been developed in the past decade, either by an end-to-end prepolymer linking process[9] or alternatively by a ring-expansion polymerization technique.[10,11] In addition, remarkable topological effects due to their cyclic forms have now been unequivocally demonstrated by making use of cyclic polymers having prescribed chemical structures.[4,12] Notably, moreover, a variety of topologically attractive, *mechanically linked* cyclic molecules, including simple trefoils to complex pentafoil knots, and a simple Hopf link, i.e., [2]-catenane, to complex Borromean rings,[13] have been constructed by taking advantage of elaborated self-assembly protocols based either on biopolymer (DNA) systems[3,14] or on noncovalent complementary interactions by tailored molecular components.[2,15]

A class of *bonded* (covalently linked) *multicyclic* polymer topologies, including three subclasses of *fused*, *spiro*, and *bridged* forms, has also been ongoing synthetic challenge in polymer chemistry.[4,8] Selected examples of *fused* multicyclic topologies are shown in Figure 1. In order to construct various multicyclic polymer topologies, we have developed an *electrostatic self-assembly and covalent fixation* (ESA-CF) protocol,[4,16] in which linear or star precursors having cyclic ammonium salt groups carrying plurifunctional carboxylate counteranions have been

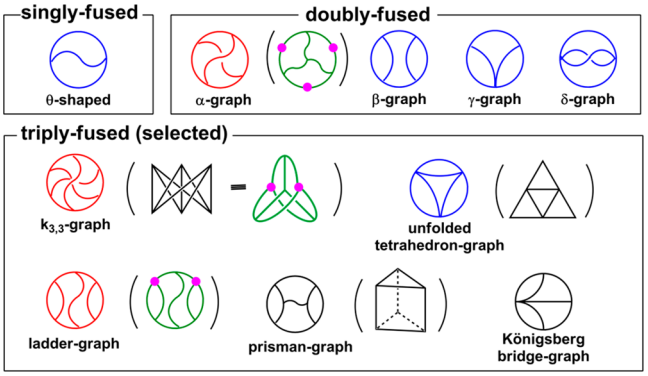

Figure 1. Graph presentation of *fused* multicyclic polymer topologies. Those in blue are so far reported, and those in red are constructed in this work. In parentheses, topologically equivalent graph constructions are also shown in black or in green, and the linking positions by the dendritic precursor used in this work are indicated in the green graphs.

employed to form polymer self-assemblies as key intermediates. All three types of dicyclic constructions, i.e., θ (*fused*), 8 (*spiro*), and manacle (*bridged*) forms have so far been constructed through the ESA-CF protocol.[16] Furthermore, single and multicyclic polymer precursors (*kyklo*-telechelics) having as large as 300-membered atom ring sizes were obtained by the ESA-CF protocol.[17] A variety of tricyclic and tetracyclic polymer topologies of *spiro*- and *bridged*-forms[18] and three doubly *fused* tricycle (δ-, γ-, and β-graph) forms,[19] as well as an example of a triply *fused* tetracyclic form (unfolded tetrahedron-graph)[20] were subsequently constructed in con-

Received: May 19, 2014
Published: June 23, 2014

   dx.doi.org/10.1021/ja504891x | J. Am. Chem. Soc. 2014, 136, 10148−10155

Scheme 1. Synthesis of a Hexafunctional Dendritic Precursor, $4/CF_3SO_3^-$

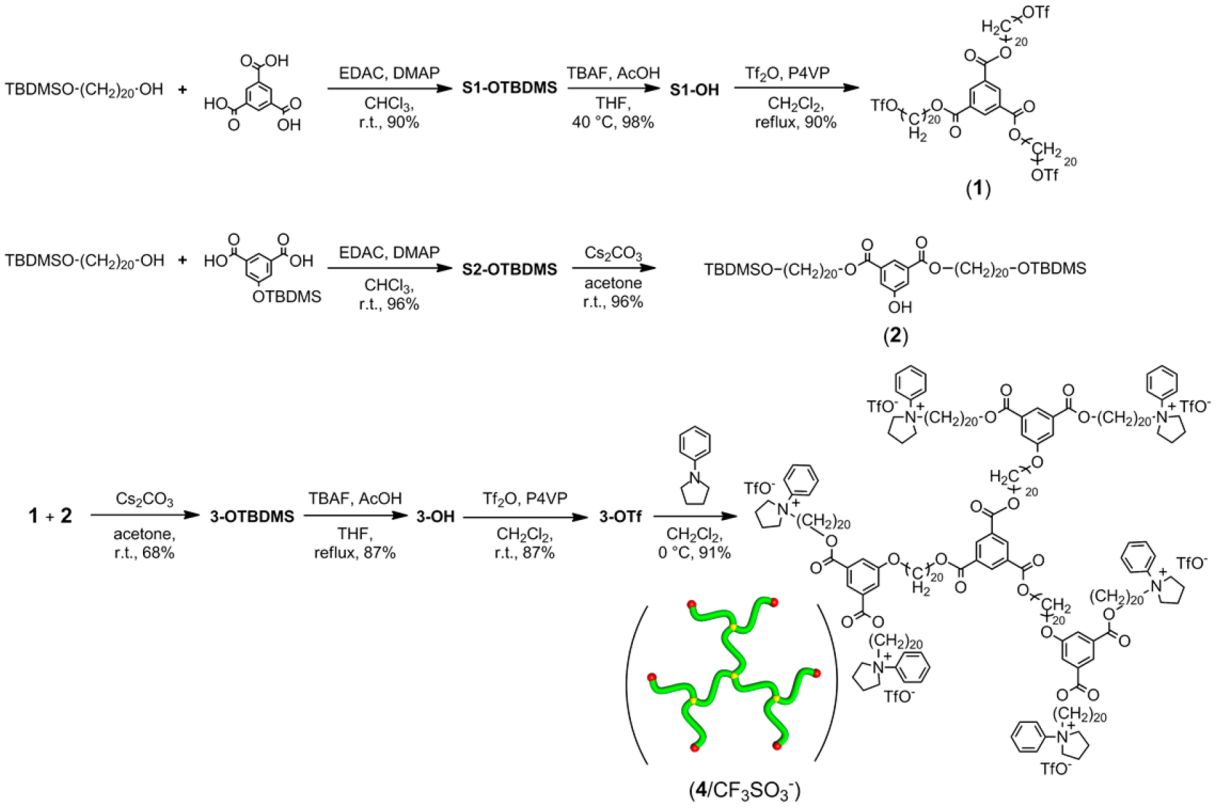

junction with a tandem alkyne−azide addition, i.e., *click*, and olefin metathesis, i.e., *clip*, reactions. Yet, a class of topologically significant *fused*-multicyclic forms, including α-graph (or K_4 graph) and, in particular, a tetracyclic $K_{3,3}$ form, shown in Figure1, have still been a challenge.[21]

The $K_{3,3}$ graph is a prototypical nonplanar graph, which cannot be embedded in the plane in such a way that its edges intersect only at their end points. Interestingly moreover, the $K_{3,3}$ graph can be drawn on the torus surface by avoiding such intersection of the edges.[4,8] In this relevance, a trefoil knot and a Hopf link (2-catenane), having three and two intrinsic intersections, respectively, are also included in a class of nonplanar graphs. Therefore, the $K_{3,3}$ graph having an intrinsic single intersection is considered as a primary form in nonplanar graph constructions. Remarkably, in nature, the $K_{3,3}$ graph topology has recently been identified in cyclic polypeptides (cyclotides) produced through the intramolecular S−S bridging with cysteine residues,[22] and their programmed folding structures are considered to be crucial for their extraordinary stability and bioactivity.[23,24] It is, therefore, inspiring to explore experimentally how such unique topological properties in basic graph theories can direct any fundamental characteristics of flexible polymer molecules. As a first step of this challenge, we demonstrate herein the successful construction of a macromolecular $K_{3,3}$ graph,[25] having uniform-size edge components of eicosanediol (C_{20}) segments.

RESULTS AND DISCUSSION

Preparation of A Dendritic Macromolecular Precursor Having Six *N*-Phenylpyrrolidinium Salt End Groups. A dendritic macromolecular precursor having six *N*-phenylpyrrolidinium salt end groups, $\mathbf{4}/CF_3SO_3^-$, was prepared through the reaction of one unit of a three-armed star-shaped molecule having triflate ester end groups, **1**, with three units of a linear molecule having a phenolic group at the center position, **2**, (Scheme 1, and detailed in Supporting Information [SI]). The star precursor, **1**, was obtained by the esterification reaction of a single-end protected 1,20-eicosanediol with trimesic acid, followed by the deprotection and the triflate esterification of the hydroxyl groups with trifluoromethanesulfonic anhydride. The linear precursor, **2**, was also obtained through the esterification of a single-end protected 1,20-eicosanediol with an isophthalic acid derivative having a protected phenolic group. The coupling reaction of the two precursors, **1** and **2**, was conducted in the presence of Cs_2CO_3 in acetone. After the deprotection, the six hydroxyl end groups of the obtained dendritic product, **3-OH**, were converted into trifluoromethanesulfonate ester groups by treatment with triflic anhydride in the presence of poly(4-vinylpyridine). Finally, quaternization with *N*-phenylpyrrolidine was conducted to produce a dendritic precursor, $\mathbf{4}/CF_3SO_3^-$.

^1H and ^{13}C NMR spectroscopic and MALDI-TOF mass analyses (Figures S1−S12 in the SI) unequivocally confirmed each step to give $\mathbf{4}/CF_3SO_3^-$. Thus, the signals for the methylene groups adjacent to the hydroxyl group were visible at 3.64 ppm in the precursors and were replaced by those for the triflate ester methylene groups at 4.54 ppm, and finally by those for the methylene groups adjacent to *N*-phenyl groups at 3.84 ppm together with the *N*-phenyl proton signals at 7.45−7.78 ppm. In addition, the obtained $\mathbf{4}/CF_3SO_3^-$ was treated with tetrabutylammonium benzoate to cause the ring-opening reaction of the pyrrolidinium salt groups. The selective formation of a covalently converted product was confirmed by ^1H and ^{13}C NMR and MALDI-TOF mass analyses of the product (Figures S13−S15 in the SI).

dx.doi.org/10.1021/ja504891x | J. Am. Chem. Soc. 2014, 136, 10148−10155

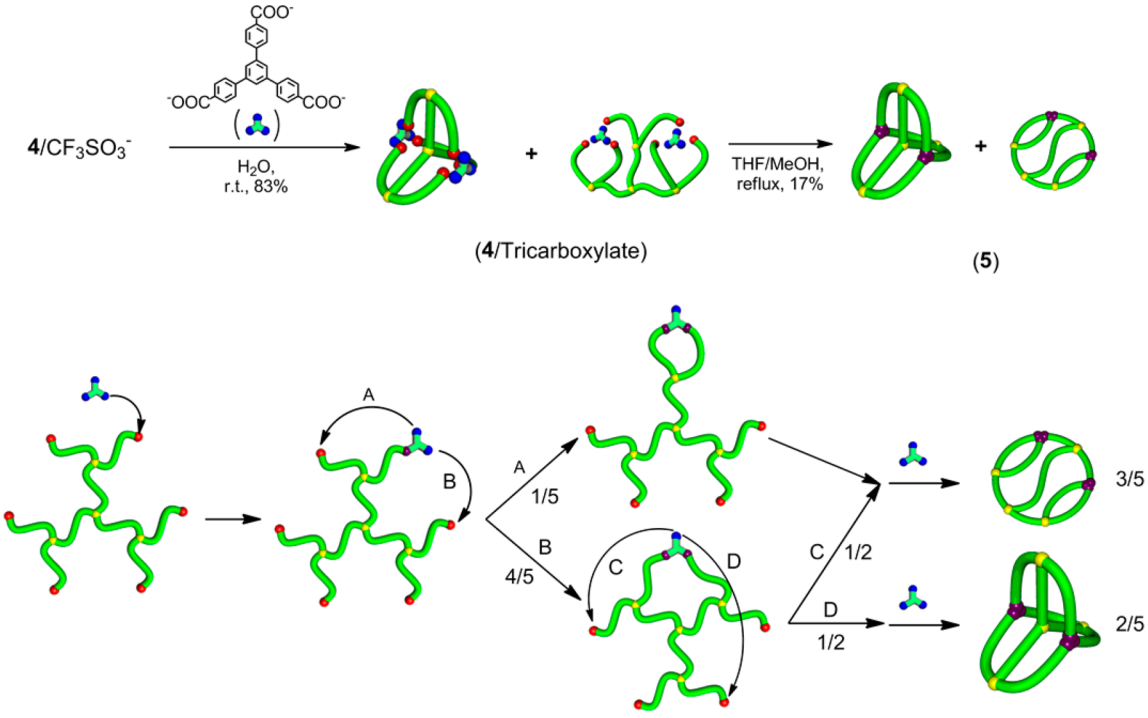

Figure 2. (top) Construction of a triply-*fused* tetracyclic polymer topologies (**5**) by the ESA-CF process with a dendritic precursor carrying two trifunctional counteranions, **4/Tricarboxylate**, and (bottom) a scheme showing random combination of the end groups during the covalent conversion of **4/Tricarboxylate**.

Constructing A Macromolecular $K_{3,3}$ Graph. The six triflate counteranions in **4/$CF_3SO_3^-$** were subsequently exchanged to two units of trifunctional carboxylate, 1,3,5-tris(4-carboxylatephenyl)benzene (Figure 2, top), through the precipitation of a THF solution of **4/$CF_3SO_3^-$** into an ice-cooled aqueous solution containing a large excess of the tricarboxylate as the Na^+ salt. The ion-exchange product, recovered with retention of a trace amount of water in order to avoid an uncontrolled ring-opening reaction, was examined by ^{1}H NMR analysis in a solvent of $CDCl_3$ with a drop of CD_3OD due to the solubility of the product (Figure 3, top), where the phenyl signals from the tricarboxylate anions appear at 7.46−7.78 ppm and at 8.10−8.12 ppm.

Significantly, the obtained electrostatic self-assembly, **4/Tricarboxylate**, tends to produce specific ion-pair forms under dilution, where the anions and the cations balance the charges in the smallest number of the components (Figure 2, top). The ionic intermediate, **4/Tricarboxylate**, was then subjected to heat treatment by refluxing in THF/CH_3OH (vol/vol = 9/1) at a concentration of 0.1 g/L for 12 h, to cause an intramolecular covalent reaction by ring-opening of the cyclic ammonium salt groups by carboxylate groups. The soluble product, **5**, was isolated after the reprecipitation into water and subsequent silica-gel column (CH_2Cl_2) workup in 17% yield (4.4 mg). The covalent conversion reaction was confirmed by the ^{1}H NMR spectroscopic analysis (Figure 3, bottom), where the signals for the methylene protons adjacent to *N*-phenyl groups visible at 3.60−3.73 ppm were replaced by the multiplet signal for the ester-methylene protons at 4.18−4.47 ppm. In addition, the signals at 7.46−7.76 ppm due to the *N*-phenyl protons observed in the ionic **4/Tricarboxylate** were replaced by those at 6.53−6.71 and 7.19 ppm after the covalent conversion. By MALDI-TOF mass analysis,[26] the covalent conversion product showed a peak at m/z = 5024.29, corresponding to the most abundant mass of the product possessing the expected chemical structure of $C_{327}H_{480}N_6O_{33}$ plus H^+ as 5023.63, which is expected, given the presence of multiple basic amine functionalities in the macromolecule and the use of a mildly acidic matrix.

Notably, a pair of constitutional isomer products, i.e., a $K_{3,3}$ graph form and another ladder-shaped counterpart, are produced during the covalent conversion of **4/Tricarboxylate**, according to the linking mode of the six chain-ends of the dendritic precursors by two units of a trifunctional reagent. A random combination should result in the two isomers in the ratio of 3:2, and the $K_{3,3}$ graph product as a minor component (Figure 2, bottom).

A preparative recycling SEC technique was successfully applied to resolve and isolate these two constitutional isomers, possessing distinctive hydrodynamic volumes in solution, confirmed by the simulation by assuming random coil conformations.[27] The presence of the two components (fractions 1 and 2, respectively) was disclosed after repeated recycling (Figure 4), but the eventual resolution was not obvious at the first cycle. The isomer ratio was 7:3 estimated from the SEC peak area, with the smaller hydrodynamic volume component (fraction 2), presumably the $K_{3,3}$ graph product, as a minor component. This is comparable with the statistical isomer ratio of 6:4, and the slight preference of the major ladder product is reasoned by its smaller ring formation path involved in the covalent conversion of **4/Tricarboxylate** (Figure 2). The resolved two components having the larger and smaller elution volumes were subsequently isolated by a stepwise fractionation after the 17th cycle. (Figure 4)

The isolated two components in **5** (fraction 1 and 2) exhibited nearly identical ^{1}H NMR (Figure 5, left, top and bottom, respectively) and MALDI-TOF mass spectra (Figure 5, right, middle, and bottom, respectively). In addition, not only

dx.doi.org/10.1021/ja504891x | J. Am. Chem. Soc. 2014, 136, 10148−10155

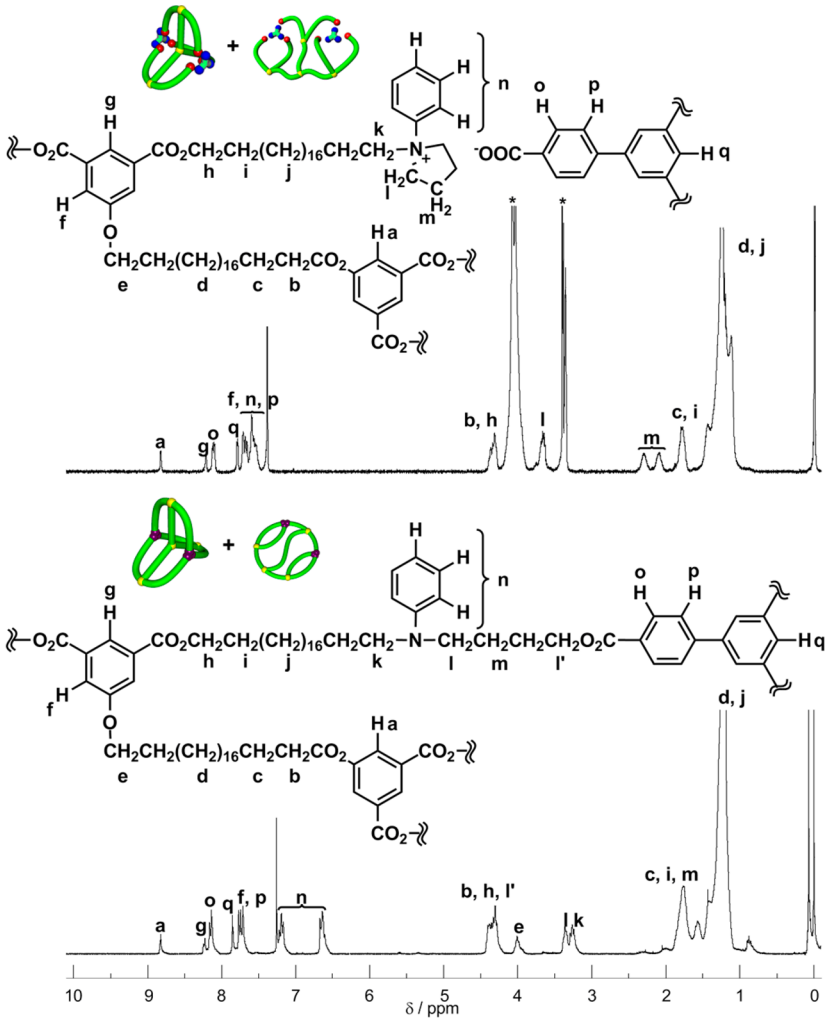

Figure 3. ^{1}H NMR (300 MHz) spectra of (top) an electrostatic self-assembly composed of a hexafunctional dendritic precursor carrying two trifunctional counteranions, **4**/**Tricarboxylate**, ($CDCl_3$/CD_3OD at 25 °C, The signals with * are due to the undeutrated fraction of CD_3OD and H_2O) and (bottom) the covalent converted product (**5**) therefrom ($CDCl_3$ at 25 °C).

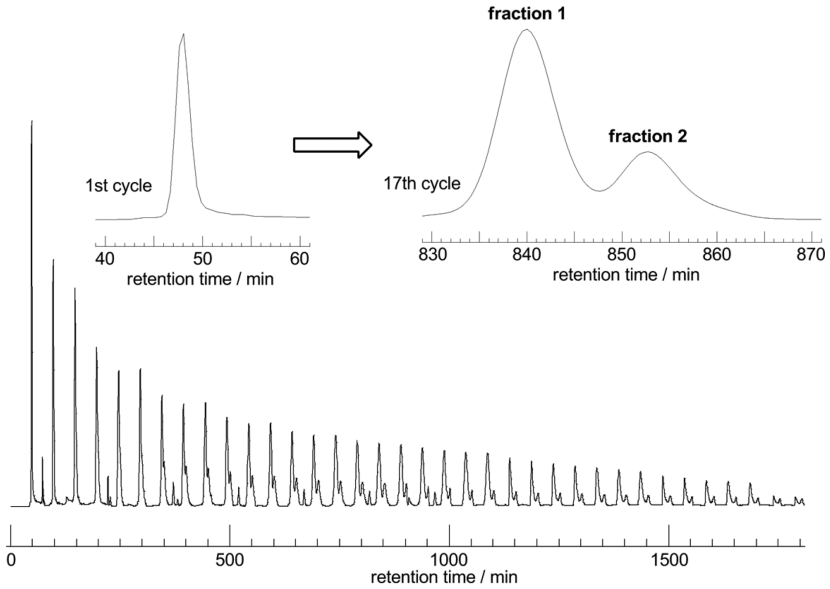

Figure 4. Recycling SEC traces for the product **5** with insets showing the first and the 17th cycle charts. ($CHCl_3$ as an eluent at a flow rate of 3.5 mL/min, fractionation/isolation started after 17th cycle.)

dx.doi.org/10.1021/ja504891x | J. Am. Chem. Soc. 2014, 136, 10148−10155

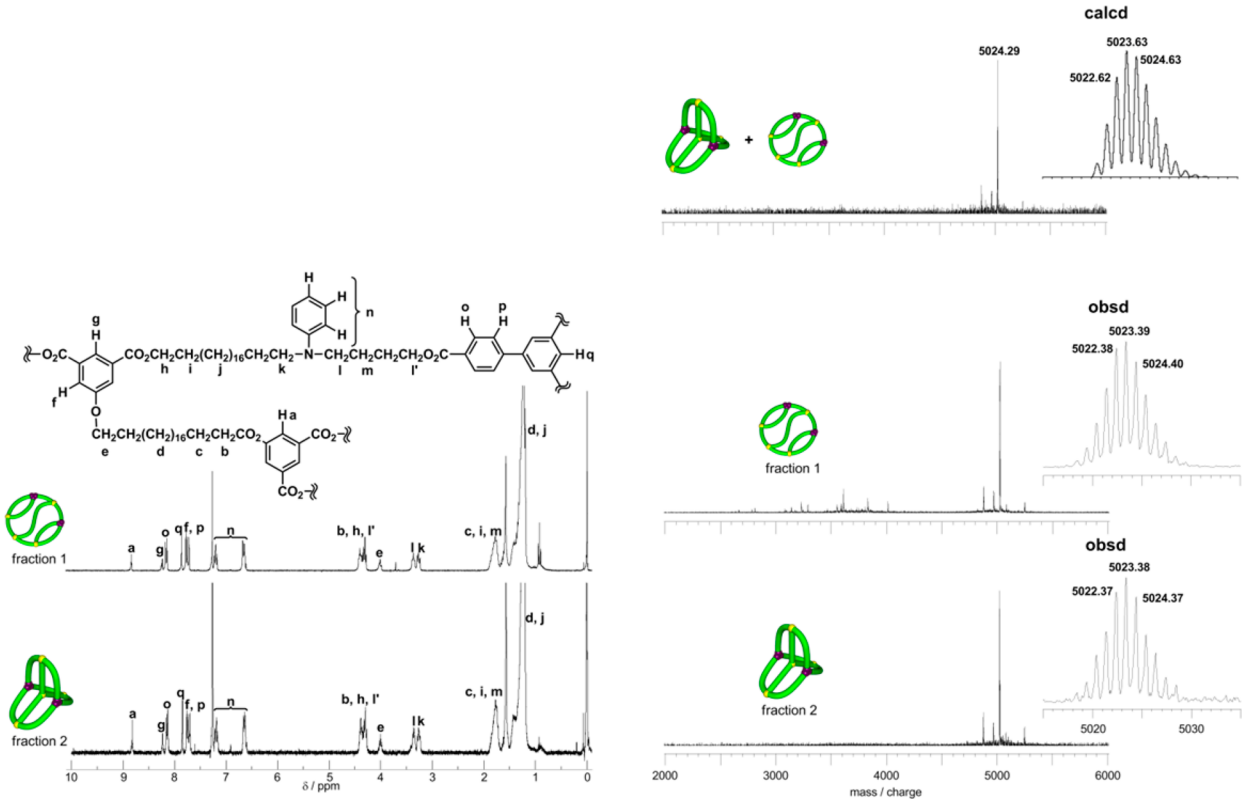

Figure 5. ^{1}H NMR spectra (left) of the isolated two components (fraction 1, top, as major and fraction 2, bottom, as minor components), and MALDI-TOF mass spectra (right) of (top) the covalent converted product **5** from **4**/**Tricarboxylate**, and (middle and bottom) the two isolated components by the SEC fractionation. (^{1}H NMR: 300 MHz, $CDCl_3$ at 25 °C; MALDI-TOF mass: linear mode, dithranol with sodium trifluoroacetate as matrix.)

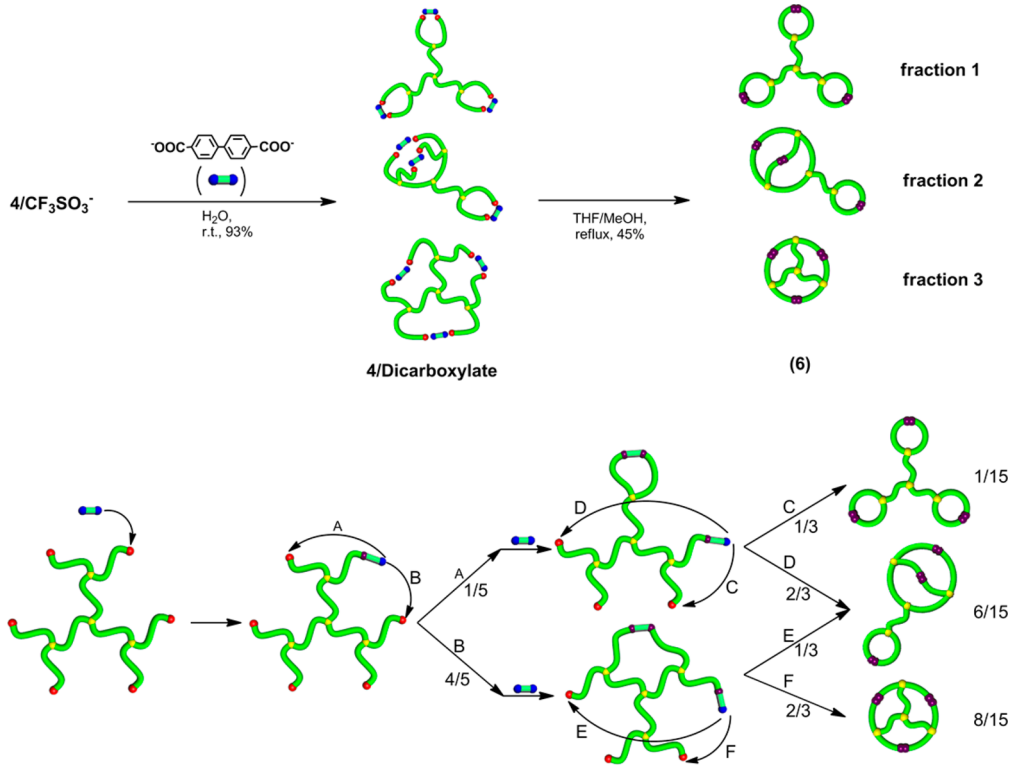

Figure 6. (top) Construction of doubly-*fused* tricyclic polymer topologies (**6**) by the ESA-CF process with a dendritic precursor carrying three difunctional counteranions, **4**/**Dicarboxylate**, and (bottom) a scheme showing random combinations of the end groups during the covalent conversion.

dx.doi.org/10.1021/ja504891x | J. Am. Chem. Soc. 2014, 136, 10148−10155

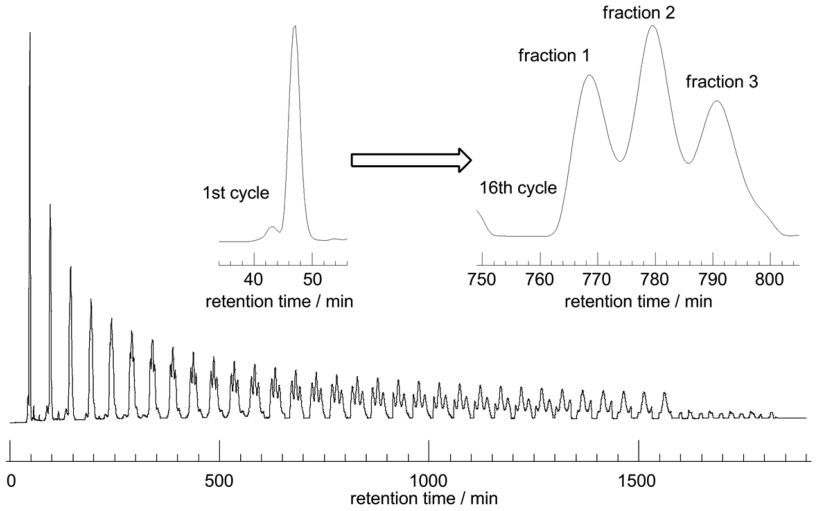

Figure 7. Recycling SEC traces for the product **6** with insets showing the first and the 16th cycle charts. ($CHCl_3$ as an eluent at the flow rate of 3.5 mL/min, fractionation/isolation started after 16th cycle.)

the observed MALDI-TOF peak molar mass but also the observed fine structures due to the isotope distribution pattern in the products exactly matched the calculated ones (Figure 5, right, top, middle and bottom, respectively). On the other hand, their hydrodynamic volumes in solution, estimated by the SEC peak molecular weights (M_p) with polystyrene standards for the calibration as a quantitative measure, i.e., M_p = 3440 and 2990,[28] respectively, were distinctly different from each other, and the hydrodynamic volume ratio of the two isomers estimated by the SEC, i.e., 2990/3440 = 0.87, was in close agreement with the simulation result of the ratio of the square of the radius of gyration (R_g^2), i.e., 0.43/0.50 = 0.86.[27] Upon these results, the minor component (fraction 2) having the smaller 3D size was reasonably assigned as the $K_{3,3}$ graph product.

Macromolecular Tricyclic Topological Isomers through Electrostatic Self-Assembly and Covalent Fixation. The ESA-CF protocol has also been applied for the construction of tricyclic macromolecular topologies, by the ion-exchange reaction between **4**/$CF_3SO_3^-$ and a difunctional carboxylate, 4,4′-biphenyldicarboxylate (Figure 6, top). Thus, the electrostatic self-assembly, **4**/**Dicarboxylate**, was subjected to the covalent conversion reaction in dilute solution to give three tricyclic constitutional isomers, including a *fused*-type α-graph topology and a *bridged*-type three-way paddle-form (Figure 6 and Figures S16−S17 in the SI). The preparative recycling SEC technique was successfully applied, as in the case of **4**/**Tricarboxylate**, to resolve and isolate the three constitutional isomer components, possessing distinctive hydrodynamic volumes in solution, which was envisaged also by the simulation.[27] The presence of three components was indeed demonstrated after repeated recycling (Figure 7), and the three isomer components were subsequently isolated by first collecting the larger and smaller elution volume components with stepwise fractionation after the 16th cycle (Figure 7). The three isolated components in **6** (fraction 1, 2, and 3, respectively) exhibited identical ^{1}H NMR (Figure S18 in the SI) and MALDI-TOF (Figure S19 in the SI) spectra, and confirmed the expected chemical structures of the three constitutional isomers. The observed isomer ratio was 3:4:3 from the SEC peak area, and the smallest hydrodynamic volume component (fraction 3) is assignable to a doubly *fused* tricyclic α-graph product. The observed isomer ratio was noticeably different from the statistical ratio of 1:6:8, (Figure 6, bottom) which is rationalized by preference for linking processes between chain-ends at structurally closer positions, as observed before in the relevant dicyclic θ and manacle isomer formation process.[29]

Finally, the analytical SEC measurement was conducted of a series of tricyclic and tetracyclic products, including a $K_{3,3}$ graph topology macromolecule, together with the starting dendritic precursor. (Figure 8) It was clearly seen that the triply *fused* tetracyclic $K_{3,3}$ graph macromolecule is significantly contracted in its 3D size, in comparison with the starting dendritic precursor and with other *spiro*- and *bridged*-multicyclic counterparts. Indeed, the hydrodynamic volume ratio of the $K_{3,3}$ graph macromolecule against the dendritic precursor (M_p = 4840), estimated by the SEC peak molecular weights, was 0.62.

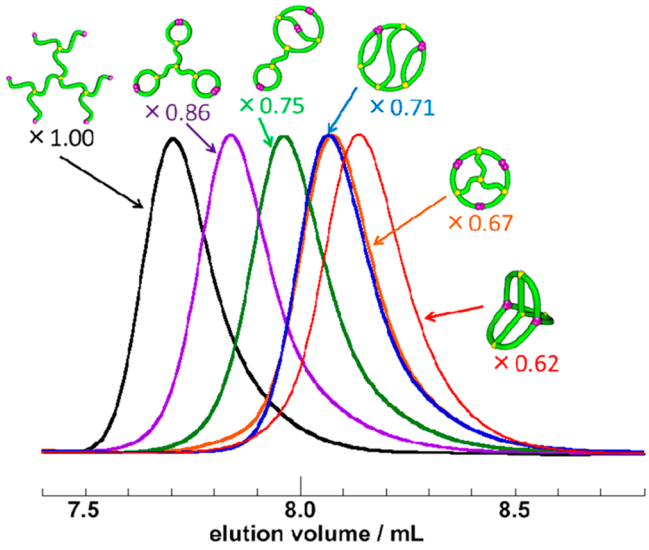

Figure 8. Analytical SEC charts of dicyclic and tricyclic polymers obtained in this study with relative hydrodynamic volumes with reference to the dendritic precursor, obtained after the covalent conversion of ionic end groups of **4**/$CF_3SO_3^-$. (THF as an eluent at the flow rate of 1.0 mL/min.)

dx.doi.org/10.1021/ja504891x | J. Am. Chem. Soc. 2014, 136, 10148−10155

This result implies the evolutional consequence of a class of cyclotides having a folded structure equivalent to the $K_{3,3}$ graph topology to realize an extremely compact 3D conformation, achieving exceptionally thermostable bioactivities. Furthermore, this work will provide new insights in polymer materials design by chain-folding, to modulate the conformational stability of randomly coiled flexible polymer segments.

■ ASSOCIATED CONTENT

Supporting Information

Detailed description of materials and methods, preparation and reaction procedures for a dendritic precursor, electrostatic self-assemblies with trifunctional and bifunctional carboxylate counterions, and covalent conversion products, as well as SEC fractionation of topological isomers, and ^{1}H NMR and MALDI-TOF mass spectra of the products. This material is available free of charge via the Internet at http://pubs.acs.org.

■ AUTHOR INFORMATION

Corresponding Author

ytezuka@o.cc.titech.ac.jp

Notes

The authors declare no competing financial interest.

■ ACKNOWLEDGMENTS

We thank Prof. T. Deguchi and Ms. E. Uehara (Ochanomizu University) for the simulation work. We also acknowledge G. Matsuura, M. Nakashima, H. Fujimoto, and F. Ando for their contributions in the initial stage of this project. This work was supported partly by KAKENHI (26288099 T.Y. and 23350050 Y.T.).

■ REFERENCES

(1) (a) *Complex Macromolecular Architectures, Synthesis, Characterization and Self-Assembly*; Hadjichristidis, N., Hirao, A., Tezuka, Y., Du Prez, F., Eds.; Wiley: Singapore, 2011. (b) *Synthesis of Polymers*; Schüter, A. D., Hawker, C. J., Sakamoto, J., Eds.; Wiley-VCH: Weinheim, 2012; Vols *1* and *2*.

(2) (a) *Supramolecular Polymer Chemistry*; Harada, A., Ed.; Wiley-VCH: Weinheim, 2012. (b) *Molecular Catenanes, Rotaxanes and Knots*; Sauvage, J.-P., Dietrich-Buchecker, C., Eds.; Wiley-VCH: Weinheim, 1999. (c) Fenlon, E. E. *Nat. Chem.* **2010**, *2*, 156−157.

(3) (a) Seeman, N. C. *Annu. Rev. Biochem.* **2010**, *79*, 65−87. (b) Seeman, N. C. *Mol. Biotechnol.* **2007**, *37*, 246−257.

(4) *Topological Polymer Chemistry: Progress of Cyclic Polymers in Syntheses, Properties and Functions*; Tezuka, Y., Ed.; World Scientific: Singapore, 2013.

(5) (a) *Cyclic Polymers*, 2nd ed.; Semlyen, J. A, Ed.; Kluwer: Dordrecht, 2001. (b) Endo, K. *Adv. Polym. Sci.* **2008**, *217*, 121−184. (c) Laurent, B. A.; Grayson, S. M. *Chem. Soc. Rev.* **2009**, *38*, 2202−2213. (d) Kricheldorf, H. R. *J. Polym. Sci., Part A: Polym. Chem.* **2010**, *48*, 251−284. (e) Grayson, S. M.; Getzler, Y. D. Y. L.; Zhang, D., Eds. Cyclic polymers: New developments, Special issue in *Reactive and Functional Polymers* **2014**; Vol. *80*.

(6) (a) Schappacher, M.; Deffieux, A. *Science* **2008**, *319*, 1512−1515. (b) Deffieux, A.; Schappacher, M. *Cell. Mol. Life Sci.* **2009**, *66*, 2599−2602. (c) Schappacher, M.; Deffieux, A. *Angew. Chem., Int. Ed.* **2009**, *48*, 5930−5933. (d) Boydston, A. J.; Holcombe, T. W.; Unruh, D. A.; Fréchet, J. M. J.; Grubbs, R. H. *J. Am. Chem. Soc.* **2009**, *131*, 5388−5389. (e) Xia, Y.; Boydston, A. J.; Grubbs, R. H. *Angew. Chem., Int. Ed.* **2011**, *50*, 5882−5885. (f) Zhang, K.; Zha, Y.; Peng, B.; Chen, Y.; Tew, G. N. *J. Am. Chem. Soc.* **2013**, *135*, 15994−15997. Remarkably, complex looped polymer topologies such as a knot have been identified in the polymer cyclization products (ref 6c).

(7) (a) Flapan, E. *When Topology Meets Chemistry. A Topological Look at Molecular Chirality*; Cambridge University Press: Cambridge, New York, 2000. (b) Walba, D. M. *Tetrahedron* **1985**, *41*, 3161−3212. (c) Chambron, J. C.; Dietrich-Buchecker, C.; Sauvage, J. P. *Top. Curr. Chem.* **1993**, *165*, 131−162.

(8) Tezuka, Y.; Oike, H. *J. Am. Chem. Soc.* **2001**, *123*, 11570−11576.

(9) For reviews covering developments in this subject, see (a) Jia, Z.; Monteiro, M. J. *Adv. Polym. Sci.* **2013**, *262*, 295−328. (b) Grayson, S. M. *Nat. Chem.* **2009**, *1*, 178−179. (c) Tezuka, Y. *Polym. J.* **2012**, *44*, 1159−1169. For recent examples, see (d) Isono, T.; Kamoshida, K.; Satoh, Y.; Takaoka, T.; Sato, S.; Satoh, T.; Kakuchi, T. *Macromolecules* **2013**, *46*, 3841−3849. (e) Lu, D.; Jia, Z.; Monteiro, M. J. *Polym. Chem.* **2013**, *4*, 2080−2089. (f) Zhu, X.; Zhou, N.; Zhu, J.; Zhang, Z.; Zhang, W.; Cheng, Z.; Tu, Y.; Zhu, X. *Macromol. Rapid Commun.* **2013**, *34*, 1014−1019. (g) Willenbacher, J.; Altintas, O.; Roesky, P. W.; Barner-Kowollik, C. *Macromol. Rapid Commun.* **2013**, *34*, 1518−1523. (h) Liu, B.; Wang, H.; Zhang, L.; Yang, G.; Liu, X.; Kim, I. *Polym. Chem.* **2013**, *4*, 2428−2431. (i) Voter, A. F.; Tillman, E. S.; Findeis, P. M.; Radzinski, S. C. *ACS Macro Lett.* **2012**, *1*, 1066−1070. (j) Wang, G.; Fan, X.; Hu, B.; Zhang, Y.; Huang, J. *Macromol. Rapid Commun.* **2011**, *32*, 1658−1663. (k) Quirk, R. P.; Wang, S.-F.; Foster, M. D. *Macromolecules* **2011**, *44*, 7538−7545. (l) Schulz, M.; Tanner, S.; Barqawi, H.; Binder, W. H. *J. Polym. Sci., Part A: Polym. Chem.* **2010**, *48*, 671−680. (m) Schappacher, M.; Deffieux, A. *Macromolecules* **2011**, *44*, 4503−4510.

(10) For ROMP ring-expansion, see (a) Bielawski, C. W.; Benitez, D.; Grubbs, R. H. *Science* **2002**, *297*, 2041−2044. (b) Xia, Y.; Boydston, A. J.; Gorodetskaya, I. A.; Kornfield, J. A.; Grubbs, R. H. *J. Am. Chem. Soc.* **2009**, *131*, 2670−2677. (c) Blencow, A.; Qiao, G. G. *J. Am. Chem. Soc.* **2013**, *135*, 5717−5725. For NHC ring-expansion, see (d) Brown, H. A.; Waymouth, R. M. *Acc. Chem. Res.* **2013**, *46*, 2585−2596. (e) Culkin, D. A.; Jeong, W.; Csihony, S.; Gomez, E. D.; Balsara, N. P.; Hedrick, J. L.; Waymouth, R. M. *Angew. Chem., Int. Ed.* **2007**, *46*, 2627−2630. (f) Shin, E. J.; Brown, H. A.; Gonzalez, S.; Jeong, W.; Hedrick, J. L.; Waymouth, R. M. *Angew. Chem., Int. Ed.* **2011**, *50*, 6388−6391. (g) Guo, L.; Lahasky, S. H.; Ghale, K.; Zhang, D. *J. Am. Chem. Soc.* **2012**, *134*, 9163−9171.

(11) For recent ring-expansion processes, see also (a) Kaitz, J. A.; Diesendruck, C. E.; Moore, J. S. *J. Am. Chem. Soc.* **2013**, *135*, 12755−12761. (b) Piedra-Arroni, E.; Ladavière, C.; Amogoune, A.; Bourissou, D. *J. Am. Chem. Soc.* **2013**, *135*, 13306−13309. (c) Reisberg, S. H.; Hurley, H. J.; Mathers, R. T.; Tanski, J. M.; Getzler, Y. D. Y. L. *Macromolecules* **2013**, *46*, 3273−3279. (d) Castro-Osma, J.; Alonso-Moreno, C.; Garcia-Martinez, J.; Fernández-Baeza, J.; Sánchez-Barba, L.; Lara-Sánchez, A.; Otero, A. *Macromolecules* **2013**, *46*, 6388−6394. (e) Kammiyada, H.; Konishi, A.; Ouchi, M.; Sawamoto, M. *ACS Macro Lett.* **2013**, *2*, 531−534.

(12) For reviews covering developments in this subject, see (a) Yamamoto, T.; Tezuka, Y. *Polym. Chem.* **2011**, *2*, 1930−1941. (b) Fox, M. E.; Szoka, F.; Fréchet, J. M. J. *Acc. Chem. Res.* **2009**, *42*, 1141−1151. (c) McLeish, T. *Nat. Mater.* **2008**, *7*, 933−935. For recent examples, see (d) Honda, S.; Yamamoto, T.; Tezuka, Y. *Nat. Commun.* **2013**, *4*, 1574. (e) Habuchi, S.; Fujiwara, S.; Yamamoto, T.; Vacha, M.; Tezuka, Y. *Anal. Chem.* **2013**, *85*, 7369−7376. (f) Ren, J. M.; Satoh, K.; Goh, T. K.; Blencowe, A.; Nagai, K.; Ishitake, K.; Christofferson, A. J.; Yiapanis, G.; Yarovsky, I.; Kamigaito, M.; Qiao, G. G. *Angew. Chem. Int.* **2014**, *53*, 459−464. (g) Stanford, M. J.; Pflughaupt, R. L.; Dove, A. P. *Macromolecules* **2010**, *43*, 6538−6541. (h) Zhang, K.; Lackey, M.; Cui, J.; Tew, G. N. *J. Am. Chem. Soc.* **2011**, *133*, 4140−4148. (i) Poelma, J. E.; Ono, K.; Miyajima, D.; Aida, T.; Satoh, K.; Hawker, C. J. *ACS Nano* **2012**, *6*, 10845−10854. (j) Lee, C.-U.; Li, A.; Ghale, K.; Zhang, D. *Macromolecules* **2013**, *46*, 8213−8223. (k) Li, L.; Yang, J.; Zhou, J. *Macromolecules* **2013**, *46*, 2808−2817. (l) Wei, H.; Chu, D. S. H.; Zhao, J.; Pahang, J. A.; Pun, S. H. *ACS Macro Lett.* **2013**, *2*, 1047−1050. (m) Pasquino, R.; Vasilakopoulos, T. C.; Jeong, Y. C.; Lee, H.; Rogers, S.; Sakellariou, G.; Allgaier, J.; Takano, A.; Brás, A. R.; Chang, T.; Goossen, S.; Pyckhout-Hintzen, W.; Wischnewski, A.; Hadjichristidis, N.; Richter, D.; Rubinstein, M.; Vlassopoulos, D. *ACS Macro Lett.* **2013**, *2*, 874−878. (n) Takeshita,

H.; Poovarodom, M.; Kiya, T.; Arai, F.; Takenaka, K.; Miya, M.; Shiomi, T. *Polymer* **2012**, *53*, 5375−5384. (o) Chen, W.; Chen, J.; Liu, L.; Xu, X.; An, L. *Macromolecules* **2013**, *46*, 7542−7549. (p) Ida, D.; Nakatomo, D.; Yoshizaki, T. *Polym. J.* **2010**, *42*, 735−744. (q) Coulembier, O.; Deshayes, G.; Surin, M.; De Winter, J.; Boon, F.; Delcourt, C.; Leclére, P.; Lazzoroni, R.; Gerbaux, P.; Dubois, P. *Polym. Chem.* **2013**, *4*, 237−241.

(13) (a) Chichak, K. S.; Cantrill, S. J.; Pease, A. R.; Chiu, S.-H.; Cave, G. W. V.; Atwood, J. L.; Stoddart, J. F. *Science* **2004**, *304*, 1308−1312. (b) Cantrill, S. J.; Chichak, K. S.; Peters, A. J.; Stoddart, J. F. *Acc. Chem. Res.* **2005**, *38*, 1−9.

(14) (a) Zhang, W.-B.; Sun, F.; Tirrell, D. A.; Arnold, F. H. *J. Am. Chem. Soc.* **2013**, *135*, 13988−13997. (b) Liu, Y.; Kuzuya, A.; Sha, R.; Guillaume, J.; Wang, R.; Canary, J. W.; Seeman, N. C. *J. Am. Chem. Soc.* **2008**, *130*, 10882−10883.

(15) (a) Ayme, J.-F.; Beves, J. E.; Campbell, C. J.; Leigh, D. A. *Chem. Soc. Rev.* **2013**, *42*, 1700−1712. (b) Clark, P. G.; Guidry, E. N.; Chan, W. Y.; Steinmetz, W. E.; Grubbs, R. H. *J. Am. Chem. Soc.* **2010**, *132*, 3405−3412. (c) Ishikawa, K.; Yamamoto, T.; Asakawa, M.; Tezuka, Y. *Macromolecules* **2010**, *43*, 168−176.

(16) Oike, H.; Imaizumi, H.; Mouri, T.; Yoshioka, Y.; Uchibori, A.; Tezuka, Y. *J. Am. Chem. Soc.* **2000**, *122*, 9592−9599.

(17) Oike, H.; Kobayashi, S.; Mouri, T.; Tezuka, Y. *Macromolecules* **2001**, *34*, 2742−2744.

(18) (a) Sugai, N.; Heguri, H.; Ohta, K.; Meng, Q.; Yamamoto, T.; Tezuka, Y. *J. Am. Chem. Soc.* **2010**, *132*, 14790−14802. (b) Ko, Y. S.; Yamamoto, T.; Tezuka, Y. *Macromol. Rapid Commun.* **2014**, *35*, 412−416.

(19) (a) Tezuka, Y.; Fujiyama, K. *J. Am. Chem. Soc.* **2005**, *127*, 6266−6270. (b) Igari, M.; Heguri, H.; Yamamoto, T.; Tezuka, Y. *Macromolecules* **2013**, *46*, 7303−7315.

(20) Sugai, N.; Heguri, H.; Yamamoto, T.; Tezuka, Y. *J. Am. Chem. Soc.* **2011**, *133*, 19694−19697.

(21) A compound having a molecular skeleton equivalent to a $K_{3,3}$ graph topology has been reported Chen, C.-T.; Gantzel, P.; Siegel, J. S.; Baldridge, K. K.; English, R. B.; Ho, D. M. *Angew. Chem., Int. Ed.* **1995**, *34*, 2657−2660.

(22) (a) Craik, D. J. *Science* **2006**, *311*, 1563−1564. (b) Craik, D. J. *Trends Plant Sci.* **2009**, *14*, 328−335. (c) Jagadish, K.; Camarero, J. A. *Biopolymers* **2010**, *94*, 611−616. (d) Craik, D. *Nat. Chem.* **2012**, *4*, 600−602.

(23) (a) Alon, A.; Grossman, I.; Gat, Y.; Kodali, V. K.; DiMaio, F.; Mehlman, T.; Haran, G.; Baker, D.; Thorpe, C.; Fass, D. *Nature* **2012**, *488*, 414−418. (b) Wu, C.; Leroux, J.-C.; Gauthier, M. A. *Nat. Chem.* **2012**, *4*, 1044−1049. (c) Jagadish, K.; Borra, R.; Lacey, V.; Majumder, S.; Shekhtman, A.; Wang, L.; Camarero, J. A. *Angew. Chem., Int. Ed.* **2013**, *52*, 3126−3131. (d) Ji, Y.; Majumder, S.; Millard, M.; Borra, R.; Bi, T.; Elnagar, A. Y.; Neamati, N.; Shekhtman, A.; Camarero, J. A. *J. Am. Chem. Soc.* **2013**, *135*, 11623−11633. (e) Yang, S.; Xiao, Y.; Kang, D.; Liu, J.; Li, Y.; Undheim, E. A. B.; Klint, J. K.; Rong, M.; Lai, R.; King, G. F. *Proc. Natl. Acad. Sci. U.S.A.* **2013**, *110*, 17534−17539.

(24) (a) de Araujo, A. D.; Mobli, M.; King, G. F.; Alewood, P. F. *Angew. Chem., Int. Ed.* **2012**, *51*, 10298−10302. (b) Cui, H.-K.; Guo, Y.; He, Y.; Wang, F.-L.; Chang, H.-N.; Wang, Y.-J.; Wu, F.-M.; Tian, C.-L.; Liu, L. *Angew. Chem., Int. Ed.* **2013**, *52*, 9558−9562.

(25) The triply-*fused* tetracyclic $K_{3,3}$ graph and ladder topologies constructed in this study are expressed as $IV_6(0,6)[0^a\text{-}0^b\text{-}0^c\text{-}0^a\text{-}0^b\text{-}0^c]$ and $IV_6(0,6)[0^a\text{-}0^b\text{-}0^c\text{-}0^c\text{-}0^b\text{-}0^a]$, respectively, according to the systematic notation (ref 8) .

(26) See Figure 5 (right, top) for a MALDI TOF mass spectrum of the product, **5**.

(27) The radius of gyrations (R_g) of the two tetracyclic and three tricyclic polymers shown in this work were estimated by the simulation according to the method outlined before (Uehara, E.; Deguchi, T. *J. Phys. A., Math. Theor.* **2013**, *46*, 345001, and Uehara, E.; Tanaka, R.; Inoue, M.; Hirose, F.; Deguchi, T. *React. Funct. Polym.* **2014**, *80*, 48−56). The relative R_g^2 values of each fractions with respect to the starting dendritic precursor were: 0.50 (fraction 1 in **5**), 0.43 (fraction 2 in **5**), 0.88 (fraction 1 in **6**), 0.66 (fraction 2 in **6**) and 0.52 (fraction 3 in **6**), respectively.

(28) See Figure 8 for SEC profiles of the fraction 1 and 2 in **5**.

(29) (a) Tezuka, Y.; Tsuchitani, A.; Oike, H. *Polym. Int.* **2003**, *52*, 1579−1583. (b) Tezuka, Y.; Tsuchitani, A.; Oike, H. *Macromol. Rapid Commun.* **2004**, *25*, 1531−1535.